Survival-associated 11-AS Events Interact with the Immune Microenvironment in Ovarian Cancer

Congbo Yue
Qilu Hospital of Shandong University
Tianyi Zhao
Qilu Hospital of Shandong University
Shoucai Zhang
Qilu Hospital of Shandong University
Yingjie Liu
Qilu Hospital of Shandong University
Guixi Zheng
Qilu Hospital of Shandong University
Yi Zhang (yizhang@sdu.edu.cn)
Qilu Hospital of Shandong University

Research Article

Keywords: Alternative splicing (AS), Percent Spliced In (PSI), OV, CTLA-4 and PD-1 blockers.

Posted Date: September 20th, 2021

DOI: https://doi.org/10.21203/rs.3.rs-885547/v1

Abstract

Alternative splicing (AS) events play a crucial role in the tumorigenesis and progression of cancer. Transcriptome data and Percent Spliced In (PSI) values of OV patients were downloaded from TCGA database and TCGA SpliceSeq. Totally we identified 1,472 AS events that were associated with survival of OV and exon skipping (ES) was the most important type. Univariate and multivariate Cox regression analysis were performed to identify survival-associated AS events and develop the prognostic model based on 11-AS events. The immune cells and different response to cytotoxic T lymphocyte associated antigen 4 (CTLA-4) and programmed cell death protein 1 (PD-1) blockers in low-risk and high-risk group of OV patients were analyzed. Ten kinds of immune cells were found up-regulated in low-risk group. Activated B cell, natural killer T cell, natural killer cell and regulatory T cell were associated with survival of OV. The patients in low-risk group had good response to CTLA-4 and PD-1 blockers treatment. Moreover, a regulatory network was established according to the correlation between AS events and splicing factors (SFs). The present study provided valuable insights into the underlying mechanisms of OV. AS events that were correlated with the immune system might be potential therapeutic targets.

Introduction

Ovarian cancer (OV) is the leading cause of gynecologic cancer-related death in developed countries, and it ranks the sixth most prevalent form of cancer worldwide. Nearly 70% of OV patients are diagnosed at an advanced stage, and the 5-year survival rate is below 30%[1,2]. It is generally believed that dysregulation of gene expression plays an important role in the occurrence and development of tumors. An increasing body of evidence suggests that through the analysis of gene expression patterns of various cancer types, diagnosis, prognostic markers and new therapeutic targets can be identified[3]. Although a large number of studies have focused on the alterations of gene expression to explore OV, the underlying molecular mechanism associated with tumorigenesis and progression and their effects on the immune microenvironment remain largely unexplored.

Alternative splicing (AS) events constitute a prevalent mechanism in expanding the genetic diversity of eukaryotic cells. Spatiotemporal expression profiles of AS transcripts substantially contribute to cell differentiation, specification, and organogenesis[4]. In 1977, Phillip Sharp and Richard Roberts discovered the concept of “split genes” almost at the same time. Since then, AS events have been found to play important roles in many human diseases, including cancer. Several studies have identified that AS events were associated with the occurrence, development, and metastasis of multiple types of cancers[5–8]. These findings suggest that AS events are valuable targets for cancer diagnosis, treatment, and prognosis prediction. AS events have been reported closely related to tumor microenvironment (TME) which is a very complex system. TME is composed of tumor cells, immune and inflammatory cells, tumor-related fibroblasts, stromal tissues, and various cytokines and chemokines[9–11]. AS events is ubiquitous: 60% of genes showed frequent AS isoforms in T or B lymphocytes[12]. AS-influenced immune processes have captured great attention. With the development of next-generation sequencing technologies and the

construction of The Cancer Genome Atlas (TCGA) database, the integrative analysis of RNA-sequencing data and prognosis information of patients makes it possible to systematically analyze the survival-related AS events in several types of cancers[13]. The prognostic values of AS events have been reported in patients with glioblastoma, breast cancer, lung cancer, and so on[14]. The correlation between survival-associated AS events and the immune microenvironment have also been confirmed in endometrial cancer, stomach adenocarcinoma, pancreatic cancer and so on[9,15,16]. Furthermore, dysregulated splicing factors (SFs) have been reported to cause global alteration of AS events in cancer[3]. In OV, a few studies have reported AS events by comparing cancer tissues with normal tissues[1,17,18]. However, the comprehensive pattern of AS events and the relationship between survival-associated AS events and immune microenvironment in OV has not been elucidated. With the development of tumor immunotherapies, two antibodies that targets the T cell checkpoint protein CTLA-4 and PD-1 have shown remarkable clinical effects[19]. However, there are few studies on treatment efficiency of CTLA-4 and PD-1 blockers in OV.

In the present study, we conducted systematic profiling of genome-wide AS events in OV patients, which included 544 OV cases that were shared in TCGA SpliceSeq database and RNA-seq expression spectra. Moreover, we studied the relationship between aberrant AS events and the prognosis of OV patients. Then Univariate and Multivariate Cox regression analyses were used to identify survival-associated AS events and build a prognostic model based on 11-AS events. The Kaplan-Meier (K-M) curve and receiver operating characteristic (ROC) curve were performed to demonstrate the prognostic value of the prognostic model. Furthermore, we used the clinical data from TCGA database to explore the relationship between AS events and clinical features. Besides, the distribution of immune cells in OV patients between the high- and low-risk groups were displayed. We also conducted K-M survival curves to explore the immune cells associated with prognosis. The immunotherapy score (IPS) of CTLA-4 and PD-1 blockers in OV patients were downloaded from The Cancer Imaging Archive (TCIA) database. We compared the immunotherapeutic effect of CTLA-4 and PD-1 blockers in the two subgroups. In addition, SFs associated with AS events were also identified, and the relationship network between AS events and SFs was established. The AS-SF correlation network revealed several hub SF genes, including DDX39B, PNN, LUC7L3, ZC3H4, and SRSF11. Collectively, our findings shed new light on the pathogenesis and immunotherapy of OV.

Materials And Methods

Data collection and processing. The RNA transcriptome profiles and clinical information of the OV cohorts were retrieved from TCGA database[20], while the Percent-spliced-in (PSI) data of AS events were obtained from TCGA SpliceSeq database. PSI values ranging from 0 to 1 were used to quantify the AS events[21]. Subsequently, the AS events were annotated by combining the splicing type, ID number in the SpliceSeq, and the corresponding parent gene symbol[22]. Seven types of AS events were included in the present study, such as exon skipping (ES), mutually exclusive exon (ME), retained intron (RI), alternate promoter (AP), alternate terminator (AT), alternative donor site (AD), and alternative acceptor site (AA).

Survival-associated AS events in OV patients. A total of 544 OV patients were included in the present study. Patients with a follow-up of fewer than 90 days were excluded because these patients might die due to other factors, such as surgical complications. Univariate Cox regression was used to screen the survival-associated AS events with a P-value < 0.05[23]. Upset plots were created by UpSet R to visualize the intersections of all seven types of survival-related AS events in OV. Besides, the bubble charts were used to summarize the top 20 AS events of each type, except for the ME events, which only had eight survival-related AS events.

Construction of the prognostic model for OV patients. Lasso regression analysis was employed to select survival-associated AS events in each splicing type, which could avoid over-fitting. Then the prognostic model based on 11-AS events was constructed by multivariate Cox analysis. In downloaded PSI of AS events, 412 OV patients met the condition, which is non-null > 75%. Then they were combined with 544 OV patients who were followed for more than 90 days. A total of 384 patients were finally eligible. The risk score of the prognostic model was calculated for the prediction of OV, and the formula used for calculating the risk score for each patient was as follows: $Riskscore = \beta_{AS\ event1} \times PSI_{AS\ event1} + \beta_{AS\ event2} \times PSI_{AS\ event2} + \cdots + \beta_{AS\ eventn} \times PSI_{AS\ eventn}$. The patients were divided into two subgroups (high-risk and low-risk) according to the median risk score. There were 192 cases in each subgroup. K-M test was performed to estimate the predictive accuracy of the prognostic model. ROC curve and AUC were calculated by the “survival ROC” R package to assess the predictive power of the prognostic model. The detailed information of AS events, including the distribution of risk score, the distribution of survival time, and the expression heatmap, were also visualized.

Estimation of independent prognostic value. The risk score of the prognostic model and two important clinical features, including grade and age, were integrated into the univariate and multivariate Cox regression analyses to evaluate whether these features could be used as independent risk factors.

Validation the survival correlation between prognostic model and immune cells in patients with OV. Single-sample Gene Set Enrichment Analysis (ssGSEA) was used to calculate immune score to predict the level of immune cells in OV tissues[24]. Then we screened the immune cells related to survival-associated AS events. A total number of 23 immune cells and 259 patients were included for further analysis. Patients were separated into two (high/low) risk groups by the median value based on the risk score calculated by prognostic model. The R package was used to compare the distribution of immune cells between the two groups. Then we chose activated B cell for Pearson correlation analysis with other 6 kinds of cells which showed significant differences between the two groups using Graphad prism 8. K-M survival curves for survival-related immune cells were also performed in OV patients.

IPS predicts response to immunotherapy with CTLA-4 and PD-1 Blockers in OV patients. The IPS of CTLA-4 and PD-1 blockers in 260 OV patients were downloaded from the TCIA database. These 260 patients also were classified into low- and high-risk groups according to risk score of the prognostic model. Then we compared the distribution of IPS of CTLA-4 and PD-1 blockers between the two groups using R package. A violin diagram was used to visualize the different treatments response between two groups.

Potential correlation network of survival-associated AS and SFs. SFs can regulate AS events by binding to pre-mRNAs, affecting exon selection and choice of splicing site[25]. To analyze the correlation between survival-associated AS events and SFs, a regulatory network was constructed between SF genes and AS events. The expression data of SFs were extracted from TCGA database. The correlation between the SFs and these survival-associated AS events was analyzed using Pearson's correlation test. The AS-SF correlation network was plotted and visualized using the Cytoscape (3.7.1) software.

Functional enrichment analysis. To further explore the underlying mechanisms of AS in OV, we identified corresponding SF genes of AS events. Functional enrichment analysis was carried out using the Database for Annotation, Visualization, and Integrated Discovery (DAVID) online functional annotation tool. GO terms and KEGG pathways with $P < 0.05$ were considered a statistically significant difference. The SFs related to survival-associated AS events were selected as candidates for GO and KEGG pathway enrichment analysis. Both GO analysis and KEGG analysis were conducted using R x64 3.6.1 software.

Results

Details of AS events. A total of 544 OV patients were included in the present study, and 47,922 AS events in 21,794 gene symbols were identified (Supplementary Table 1). The AS events consisted of 3,995 AAs in 2,770 genes, 3,494 ADs in 2,386 genes, 9,652 APs in 3,889 genes, 8,438 ATs in 3,685 genes, 19,197 ESs in 6,916 genes, 207 MEs in 201 genes, and 2,939 RIs in 1,947 genes (Fig. 1A). The results showed that ES was the main splicing pattern, while ME was the least frequent event among the seven types of AS events in OV patients. It was important to note that the number of AS events far exceeded the number of genes. Figure 1B shows that one gene could undergo up to five types of AS events.

Survival-associated AS events. We identified 1,472 AS events using the AS event profiles in the OV cohort, which were significantly associated with overall survival (OS) of OV patients by univariate Cox regression analysis ($P < 0.05$). Figure 2A lists the number of each type of AS event. To better visualize the intersection, an UpSet plot was created as shown in Fig. 2B, and we found that up to three survival-associated AS events could occur in the same gene. Specifically, ES, AP, AT, AA, AD, and RI were all significantly linked to the OS of patients. Figure 2C indicates the AS events that were associated with survival of patients (red dots) and not associated with survival of patients (blue dots), showing that most AS events were significantly associated with patients' survival. Figure 2D-J showed the top 20 most significant survival-associated AS events of each type. For ME events, only eight AS events were related to survival.

Prognostic model selection and survival analysis. Lasso regression analysis was performed to avoid over-fitting and exclude the co-expressed AS events, which were selected by Univariate Cox analysis. Supplementary Fig. 1 presents the result of Lasso regression analysis of survival associated AS events, and we selected the most highly correlated AS events. Multivariate Cox analysis was then used to construct predictive model and calculate the risk score. Table 1 lists the prognostic model of 11-AS events. Patients were then divided into high-risk and low-risk subgroups according to the median risk

score of the prognostic model. There were 192 cases in each subgroup and the median risk score was 0.9137. According to K-M survival analysis, we found that the prognostic model played significant roles in distinguishing good or poor outcomes of patients (Fig. 3A). We plotted the ROC curve and calculated the AUC to verify the efficiency of the predictor. The result revealed that the AUC of 11-AS events was 0.733 (Fig. 3B). Supplementary Fig. 2 illustrated the distribution of patients' survival status (A), risk score (B), and the expression heatmap (C) of the prognostic model. The risk curve showed the result of patients ranking based on the risk score. There was a difference between the high-risk group and the low-risk group in risk score. The survival status of patients disclosed that there were higher mortality rates in the high-risk group (green dots represent survival, and red dots represent death). The color transition from green to red in the heat map indicated that the PSI score of the AS events was increased from low to high.

Estimation of independent prognostic value. We used Univariate and Multivariate Cox regression analyses to estimate the independent prognostic value of age, grade, and risk score of the prognostic model. Univariate Cox regression and Multivariate Cox regression analysis indicated that both age and risk score could predict survival of OV patients and were independent prognostic predictor (Fig. 4).

The tumor immune microenvironment was closely related to the prognosis of OV patients. We divided 259 patients into two groups based on the risk score calculated by prognostic model (low: 132 patients, high: 127 patients). Then the immune infiltration of the 23 immune cells were compared in these two subgroups. The proportion of 10 immune cells was significantly higher in low-risk group, including activated B cell, activated CD8 T cell, CD56 bright natural killer cell, immature B cell, MDSC, natural killer T cell, natural killer cell, regulatory T cell, T follicular helper cell and type 1 T helper cell (Fig. 5A). The correlation analysis showed that activated B cell was positively correlated with activated CD8 T cell, CD56 bright natural killer cell, immature B cell, MDSC, natural killer cell and type 1 T helper cell (Fig. 5B-G). Then we conducted K-M survival curves on these 10 kinds of immune cells and found four types of cells, including activated B cell, natural killer cell, natural killer T cell and regulatory T cell, which were associated with prognosis of OV patients (Fig. 6). We also found that high expression of activated B cell and natural killer T cell was beneficial to the prognosis of patients, while natural killer cell and regulatory T cell was on the contrary.

The response of immunotherapy with CTLA-4 and PD-1 Blockers in OV patients. We compared the IPS of CTLA-4 and PD-1 blockers in OV patients of high and low risk groups. The results indicated that the patients in low-risk group had good response to the single and combined use of the two drugs (Fig. 7).

Correlation network of SFs. To analyze the correlation between survival-associated AS events and SFs, an AS-SF network was constructed based on the result of Pearson's correlation test. Figure 8A showed that the network contained 56 SFs (blue triangles) and 104 survival-associated AS events, including 45 down-regulated AS events and 59 up-regulated AS events (red and green dots). The green lines represented AS events, which were positively correlated with the expressions of SFs, while red lines indicated negative correlations.

Interestingly, we found that MSI1 could positively regulate TACC2-13336-AP and negatively regulate TACC2-13333-AP. A total of 359 OV tumor tissues were used to show the correlation between expression of MSI1 and PSI value of TACC2-13336-AP (r = 0.6579, P < 0.0001), TACC2-13333-AP (r=-0.6554, P < 0.0001) (Fig. 8B).

GO functional and KEGG pathway enrichment analyses of OV patients. GO analysis demonstrated that “mRNA splicing via spliceosome”, “regulation of RNA splicing”, “mRNA processing”, “RNA processing”, and “regulation of alternative mRNA splicing via splicesome” were the most significant biological process terms. Moreover, “nucleoplasm”, “membrane”, “catalytic step 2 splicesome”, and “nuclear speck” were the most three significant cellular component terms. Besides, “poly (A) RNA binding”, “nucleotide binding”, and “ATP binding” were the most three significant molecular function terms (Fig. 9A). KEGG analysis revealed four remarkably enriched pathways, including “spliceosome”, “RNA transport”, “mRNA surveillance pathway”, and “RNA degradation”. It also revealed that these genes were mainly involved in the “spliceosome” pathways (Fig. 9B).

Discussion

AS event is one of the main engines driving proteome diversity. It is estimated that up to 94% of genes are alternatively spliced in humans. Just as many other cellular processes are modified during cellular growth, differentiation, and tissue development, AS events are also affected[26]. AS allows cells to generate diverse mRNA by modifying mRNA isoforms. The plasticity of AS is often exploited by cancer cells to produce isoform switches that promote cancer cell survival, proliferation, metastasis, and drug resistance. In recent years, it has been proved that AS events play an important role in the occurrence and development of several types of tumors. For example, AS event of TCF-4 is found to inhibit the proliferation and metastasis of lung cancer cells[27].TP53, FAS, CASP9, and BCL2L1 are also associated with the apoptosis and survival of cancer cells[28]. Calabretta's study has revealed that modulation of the pyruvate kinase gene (PKM) splicing can promote gemcitabine resistance in pancreatic cancer cells[29]. Recently, with the development of bioinformatics technology, TCGA project contains a large amount of RNA-seq data, PSI value of AS events, and clinical information of patients, which provides a rich source for the exploration of the relationship between AS events and the prognosis of cancer patients[27–29]. Associations between AS events and prognosis of patients have been demonstrated in non-small cell lung cancer (NSCLC), adrenocortical carcinoma (AC), head and neck squamous cell carcinoma (HNSCC), and so on. Previous studies have demonstrated the role of several AS patterns in OV. Dutta et al. have reported that EVI1 is frequently aberrantly spliced in OV, and the dominant form of EVI1 (EVI1$^{Del190–515}$) plays oncogenic roles in the tumorigenesis of OV[30]. Sosulski et al. have reported that CD44 variants containing exons v8–10 (CD44 v8–10) are associated with metastasis and worse prognosis in OV[31]. Although these reports provide evidence for the involvement of AS events in OV, it is still urgently necessary to systematically analyze the characteristics of AS events, which may provide potential prognostic biomarkers and therapeutic targets.

To explore the prognostic significance of AS events, we identified survival related AS events and constructed predictive model for OV. In the present study, we systematically described the AS profiles and explored the interaction network between AS events and SFs in OV. A total of 47,922 AS events of 21,794 genes were detected, indicating that AS was a common process in OV. ES events were the main type, accounting for 1/3 of the total AS events. AP events were the second most frequently occurring type, followed by AT events. Next, Lasso regression and Multivariate Cox regression analysis were performed to construct the prognostic model. These OV patients from TCGA database were then divided into low-risk and high-risk groups according to the risk score. K-M analysis demonstrated that the difference in OS between the low-risk patients and high-risk patients was significant. The results revealed that the risk score of the prognostic model consisting of 11 survival-related AS events had a prognostic power with an AUC of 0.733.

Immune cells in tumor microenvironment are also accompanied by the tumorigenesis and progression of cancer. More and more studies have reported that the products of AS events in cancer cells were also affected the immune system[24,32]. So AS events also have shown potential immunotherapy prospects, but how AS events affected the immune system of OV patients and whether AS events could be a target for diagnosis and therapy remain unclear. Hoyos, L. E.'s study has shown that T lymphocytes recognized neoepitopes derived from abnormal AS events to induce antitumor immune response[33]. Thus, we analyzed the association between the risk score based on 11 survival-related AS events and 23 immune cells in the immune microenvironment. The result showed that a low-risk score was significantly associated with upregulated activated B cell, activated CD8 T cell, CD56bright natural killer cell, immature B cell, MDSC, natural killer T cell, natural killer cell, regulatory T cell, T follicular helper cell and type 1 T helper cell. Activated B cell, natural killer T cell, natural killer cell and regulatory T cell. We also found there were correlations between these immune cells through correlation analysis. Activated B cell, activated CD8 T cell, natural killer cell, natural killer T cell and regulatory T cell were also associated with prognosis of OV patients according to K-M survival curves. Several previous immunotherapy studies have demonstrated that efficiency of CTLA-4 and PD-1 blockers has been shown not only in melanoma, but also in nine different tumor types[34,35]. We downloaded the IPS of CTLA-4 and PD-1 blockers in 260 OV patients from the TCIA database. The result showed that the patients in low-risk group had better response to the CTLA-4 and PD-1 blockers.

An interaction network between AS events and SFs was also established. The network contained 56 SFs and 104 survival-associated AS events (including 59 up-regulated AS events and 45 down-regulated AS events). Previous studies have shown that a single gene could regulate multiple AS events of the same parental gene, even in opposite way. Interestingly, our results indicated that MSI1 could positively regulate TACC2-13336-AP and negatively regulate TACC2-13333-AP which was consistent with previous reports.

Besides, GO functional enrichment and KEGG pathway analysis for the SFs significantly related to AS events provided helpful clues to elucidate the underlying mechanism of AS events in OV patients. According to the results, "mRNA splicing via spliceosome", "regulation of RNA splicing", "mRNA processing", "RNA processing", and "regulation of alternative mRNA splicing via splicesome" were the

most significant biological process terms. Moreover, “nucleoplasm”, “membrane”, and “catalytic step 2 splicesome” were the most three significant cellular component terms. Besides, “poly(A) RNA binding”, “nucleotide binding”, and “ATP binding” were the most three significant molecular function terms. KEGG pathway analysis revealed that these genes were mainly involved in the “spliceosome” pathways.

Although our predictor performed well in prognosis prediction of OV, there were inevitably several limitations in the current study. First of all, the data we collected from public databases were limited. Therefore, the clinical information was not comprehensive and might cause potential bias and errors. Second, our exploration of the mechanisms was not deep enough, and further studies, such as molecular and clinical trials, are necessary to confirm these findings. Our data revealed the prognostic value of survival-associated AS events and related SFs, which might play essential roles in tumor initiation and progression by regulating the corresponding AS events. Collectively, our findings might provide valuable insights into effective therapies using AS events for OV.

Data Access. The RNA transcriptome profiles and clinical information of the OV cohorts were downloaded from the TCGA database. The IPS of CTLA-4 and PD-1 blockers in OV patients were downloaded from the TCIA database.

Declarations

Authors' contributions

GXZ conceived the concept. CBY and GXZ analyzed the data and wrote the manuscript. YJL, SCZ and TYZ downloaded the TCGA data and plotted certain figures. YZ helped interpret the data and provided professional advices. All of the authors have read and approved the final manuscript.

Funding

This work was supported by grants from Key Research and Development Project of Shandong Province (2019GSF108034); National Natural Science Foundation of China (Grant No.81972005); Natural Science Foundation of Shandong Province (ZR2017MH044); Establishment of circulating nucleic acid second-generation sequencing technology platform and screening of candidate molecular targets (6010119015).

Competing Interest Statement

The authors declare no competing interests

References

1 Sergio Juárez-Méndez, A. Z.-D., Vanessa Villegas-Ruíz,Oscar Alberto Pérez-González,Mauricio Salcedo, Ricardo López-Romero, Edgar Román-Basaure, Minerva Lazos-Ochoa,Víctor Edén Montes de Oca-Fuentes,4 Guelaguetza Vázquez-Ortiz,and José Moreno. Splice variants of zinc finger protein 695 mRNA associated to ovarian cancer. *journal of Ovarian Research* **6**, 1-10 (2013).

2 Rojas, V., Hirshfield, K. M., Ganesan, S. & Rodriguez-Rodriguez, L. Molecular Characterization of Epithelial Ovarian Cancer: Implications for Diagnosis and Treatment. *Int J Mol Sci***17**, doi:10.3390/ijms17122113 (2016).

3 Zhu, J., Chen, Z. & Yong, L. Systematic profiling of alternative splicing signature reveals prognostic predictor for ovarian cancer. *Gynecol Oncol***148**, 368-374, doi:10.1016/j.ygyno.2017.11.028 (2018).

4 Lin, J. C. Impacts of Alternative Splicing Events on the Differentiation of Adipocytes. *Int J Mol Sci***16**, 22169-22189, doi:10.3390/ijms160922169 (2015).

5 Bonnal, S., Vigevani, L. & Valcárcel, J. The spliceosome as a target of novel antitumour drugs. *Nature Reviews Drug Discovery***11**, 847-859, doi:10.1038/nrd3823 (2012).

6 de Miguel, F. J. *et al.* Identification of alternative splicing events regulated by the oncogenic factor SRSF1 in lung cancer. *Cancer Res***74**, 1105-1115, doi:10.1158/0008-5472.CAN-13-1481 (2014).

7 Padgett, R. A. New connections between splicing and human disease. *Trends Genet***28**, 147-154, doi:10.1016/j.tig.2012.01.001 (2012).

8 Pajares, M. J. *et al.* Alternative splicing: an emerging topic in molecular and clinical oncology. *The Lancet Oncology***8**, 349-357, doi:10.1016/s1470-2045(07)70104-3 (2007).

9 Ye, Z. S. *et al.* Survival-associated alternative splicing events interact with the immune microenvironment in stomach adenocarcinoma. *World J Gastroenterol***27**, 2871-2894, doi:10.3748/wjg.v27.i21.2871 (2021).

10 Frankiw, L., Baltimore, D. & Li, G. Alternative mRNA splicing in cancer immunotherapy. *Nat Rev Immunol***19**, 675-687, doi:10.1038/s41577-019-0195-7 (2019).

11 Brosseau, J. P. *et al.* Tumor microenvironment-associated modifications of alternative splicing. *Rna***20**, 189-201, doi:10.1261/rna.042168.113 (2013).

12 Ergun, A. *et al.* Differential splicing across immune system lineages. *Proceedings of the National Academy of Sciences of the United States of America***110**, 14324-14329, doi:10.1073/pnas.1311839110 (2013).

13 Martinez-Montiel, N., Rosas-Murrieta, N. H., Anaya Ruiz, M., Monjaraz-Guzman, E. & Martinez-Contreras, R. Alternative Splicing as a Target for Cancer Treatment. *Int J Mol Sci***19**, doi:10.3390/ijms19020545 (2018).

14 Sveen, A., Kilpinen, S., Ruusulehto, A., Lothe, R. A. & Skotheim, R. I. Aberrant RNA splicing in cancer; expression changes and driver mutations of splicing factor genes. *Oncogene***35**, 2413-2427, doi:10.1038/onc.2015.318 (2016).

15 Liu, X. *et al.* Identification of Tumor Microenvironment-Related Alternative Splicing Events to Predict the Prognosis of Endometrial Cancer. *Front Oncol***11**, 645912, doi:10.3389/fonc.2021.645912 (2021).

16 Wang, L. *et al.* Prognostic alternative splicing signature reveals the landscape of immune infiltration in Pancreatic Cancer. *J Cancer***11**, 6530-6544, doi:10.7150/jca.47877 (2020).

17 Klinck, R. *et al.* Multiple alternative splicing markers for ovarian cancer. *Cancer Res***68**, 657-663, doi:10.1158/0008-5472.CAN-07-2580 (2008).

18 Song, J. *et al.* Systematic analysis of alternative splicing signature unveils prognostic predictor for kidney renal clear cell carcinoma. *J Cell Physiol***234**, 22753-22764, doi:10.1002/jcp.28840 (2019).

19 Charoentong, P. *et al.* Pan-cancer Immunogenomic Analyses Reveal Genotype-Immunophenotype Relationships and Predictors of Response to Checkpoint Blockade. *Cell Rep***18**, 248-262, doi:10.1016/j.celrep.2016.12.019 (2017).

20 Xie, Z. C., Wu, H. Y., Dang, Y. W. & Chen, G. Role of alternative splicing signatures in the prognosis of glioblastoma. *Cancer Med***8**, 7623-7636, doi:10.1002/cam4.2666 (2019).

21 Sun, J. R. *et al.* Genome-Wide Profiling of Alternative Splicing Signature Reveals Prognostic Predictor for Esophageal Carcinoma. *Front Genet***11**, 796, doi:10.3389/fgene.2020.00796 (2020).

22 Shao, X. Y., Dong, J., Zhang, H., Wu, Y. S. & Zheng, L. Prognostic Value and Potential Role of Alternative mRNA Splicing Events in Cervical Cancer. *Front Genet***11**, 726, doi:10.3389/fgene.2020.00726 (2020).

23 Chen, P. *et al.* Comprehensive Analysis of Prognostic Alternative Splicing Signatures in Endometrial Cancer. *Front Genet***11**, 456, doi:10.3389/fgene.2020.00456 (2020).

24 Yoshihara, K. *et al.* Inferring tumour purity and stromal and immune cell admixture from expression data. *Nat Commun***4**, 2612, doi:10.1038/ncomms3612 (2013).

25 Shen, S., Wang, Y., Wang, C., Wu, Y. N. & Xing, Y. SURVIV for survival analysis of mRNA isoform variation. *Nat Commun***7**, 11548, doi:10.1038/ncomms11548 (2016).

26 Oltean, S. & Bates, D. O. Hallmarks of alternative splicing in cancer. *Oncogene***33**, 5311-5318, doi:10.1038/onc.2013.533 (2014).

27 Fan, Y. C., Min, L., Chen, H. & Liu, Y. L. Alternative splicing isoform of T cell factor 4K suppresses the proliferation and metastasis of non-small cell lung cancer cells. *Genet Mol Res***14**, 14009-14018, doi:10.4238/2015.October.29.20 (2015).

28 Paronetto, M. P., Passacantilli, I. & Sette, C. Alternative splicing and cell survival: from tissue homeostasis to disease. *Cell Death Differ***23**, 1919-1929, doi:10.1038/cdd.2016.91 (2016).

29 Calabretta, S. *et al.* Modulation of PKM alternative splicing by PTBP1 promotes gemcitabine resistance in pancreatic cancer cells. *Oncogene***35**, 2031-2039, doi:10.1038/onc.2015.270 (2016).

30 Dutta, P. *et al.* EVI1 splice variants modulate functional responses in ovarian cancer cells. *Mol Oncol***7**, 647-668, doi:10.1016/j.molonc.2013.02.008 (2013).

31 Sosulski, A. *et al.* CD44 Splice Variant v8-10 as a Marker of Serous Ovarian Cancer Prognosis. *PLoS One***11**, e0156595, doi:10.1371/journal.pone.0156595 (2016).

32 Wu, Z. *et al.* Alternative splicing implicated in immunity and prognosis of colon adenocarcinoma. *Int Immunopharmacol***89**, 107075, doi:10.1016/j.intimp.2020.107075 (2020).

33 Hoyos, L. E. & Abdel-Wahab, O. Cancer-Specific Splicing Changes and the Potential for Splicing-Derived Neoantigens. *Cancer Cell***34**, 181-183, doi:10.1016/j.ccell.2018.07.008 (2018).

34 Schadendorf, D. *et al.* Pooled Analysis of Long-Term Survival Data From Phase II and Phase III Trials of Ipilimumab in Unresectable or Metastatic Melanoma. *J Clin Oncol***33**, 1889-1894, doi:10.1200/JCO.2014.56.2736 (2015).

35 Schumacher, T. N. & Schreiber, R. D. Neoantigens in cancer immunotherapy. **348**, 69-74, doi:10.1126/science.aaa4971 %J Science (2015).

Tables

Table 1

Mutivariate Cox analysis of prognostic AS predicting overall survival

	gene symbol	Spliceseq ID	AS type	HR.95L	HR.95H	pvalue
ALL	TSEN54	43456	AA	5.29E-20	2.25E-06	0.000337526
	SMC6	52731	AP	3.31E-05	0.244173502	0.0098632
	EDNRA	70785	ES	0.000555224	0.243945187	0.00412093
	AGO2	85285	ES	4.80E-08	0.001887305	1.83E-05
	ATRIP	64664	AD	0.000520359	0.103314245	0.000270829
	FLT3LG	50941	AP	0.037905348	0.524319914	0.00346249
	CCT7	53965	ES	0.023328416	0.33048535	0.000321669
	PIGV	1300	AP	0.09617422	0.619578962	0.003004361
	CYTIP	55643	AP	4.50E-07	0.012016318	0.000251836
	ZDHHC6	13114	AA	0.00016264	0.097870088	0.00071571
	ZNF630	88950	AP	2.328594437	80.61439575	0.003794231

Figures

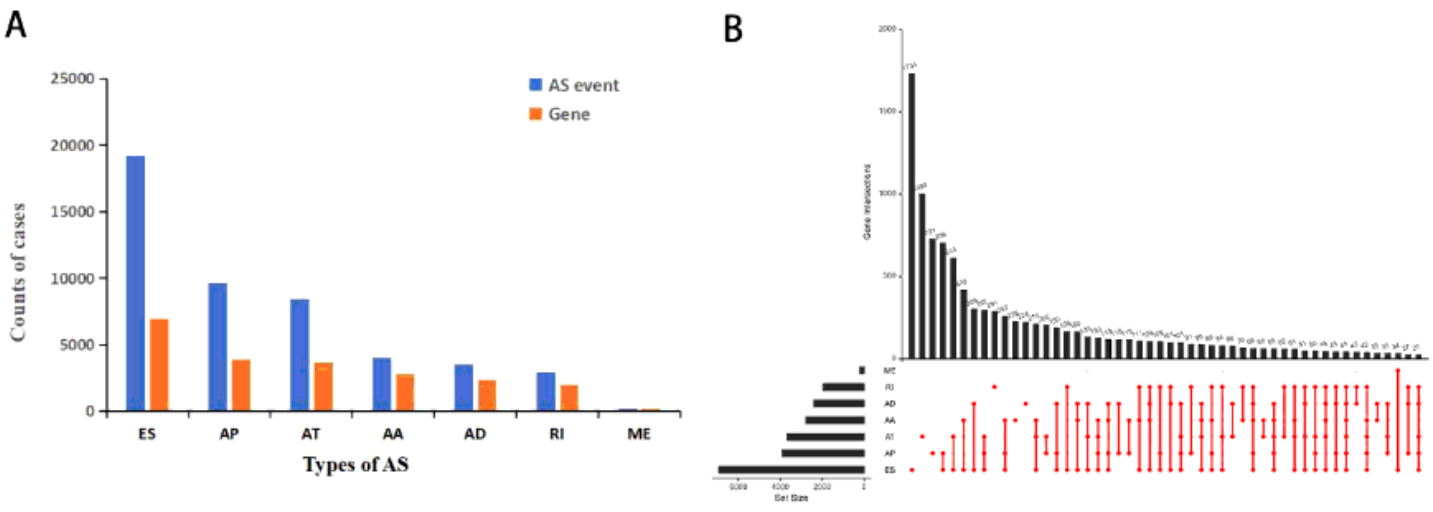

Figure 1

Summary of AS events of OV. (A) Counts of AS events and correlated genes. (B) Upset plot in OV, showing the interactions among seven types of AS events. One gene may have up to five types of AS events.

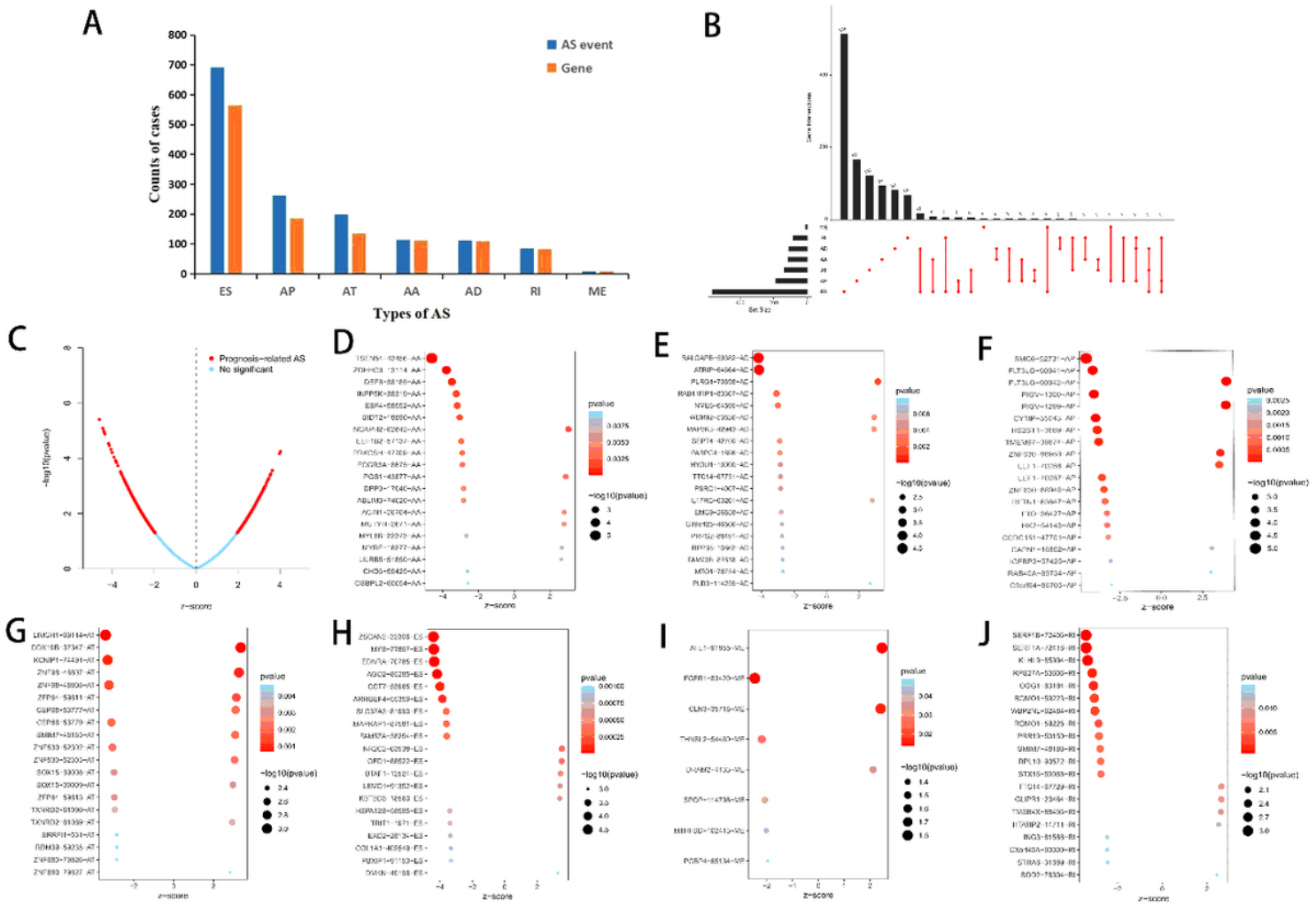

Figure 2

Top 20 significant AS events of OV. (A) Counts of survival-associated AS events and correlated genes. (B) Upset plot of interactions diagram of survival-associated AS events. (C) The volcano plot of survival-related AS events (red dots). Red dots indicate survival-related AS events in OV. Blue dots indicate AS events unrelated to survival in OV. Bubble plots of the top 20 survival-related AS events based on AA (D), AD (E), AP (F), AT (G), ES (H), ME (I), and RI (J), respectively.

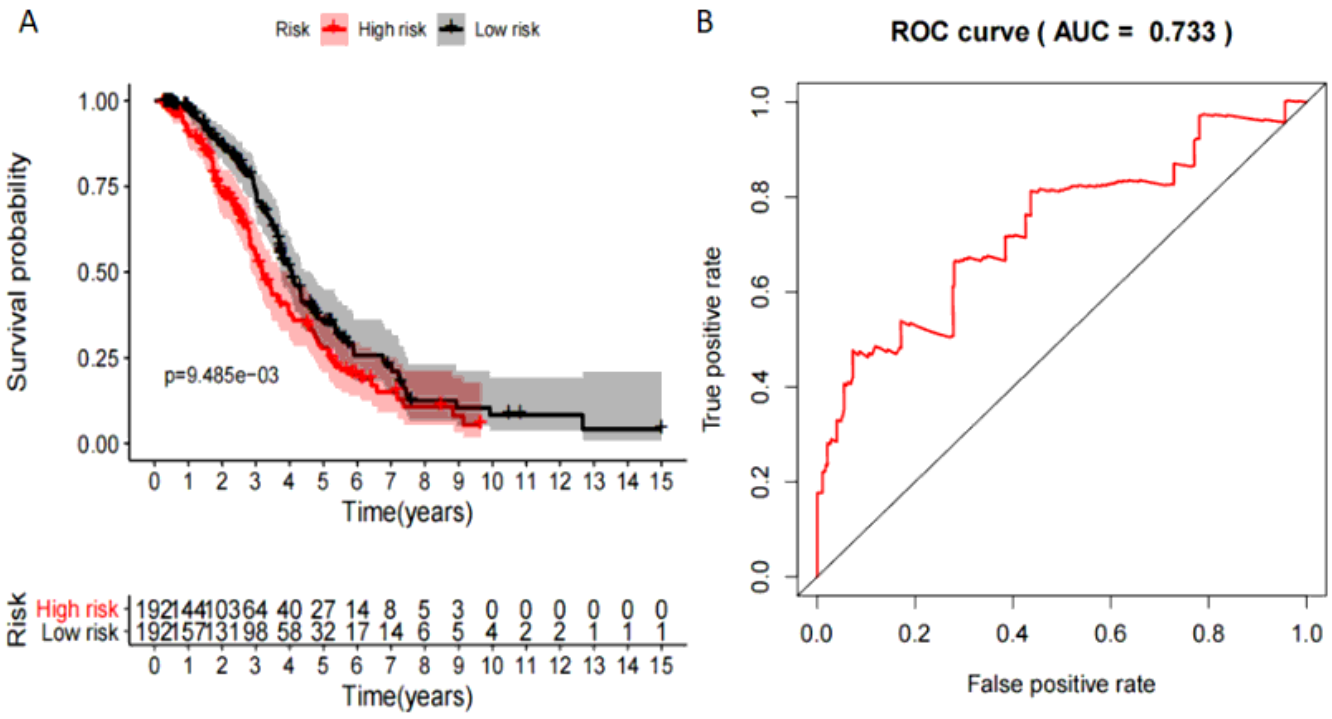

Figure 3

The K-M curve indicated the OS of high-risk patients (red line) and low-risk patients (blue line) based on 11-AS events (A). The ROC curve evaluated the predictive power of prognostic model and the risk score reflected the greatest prognostic power with an AUC of 0.733 (B).

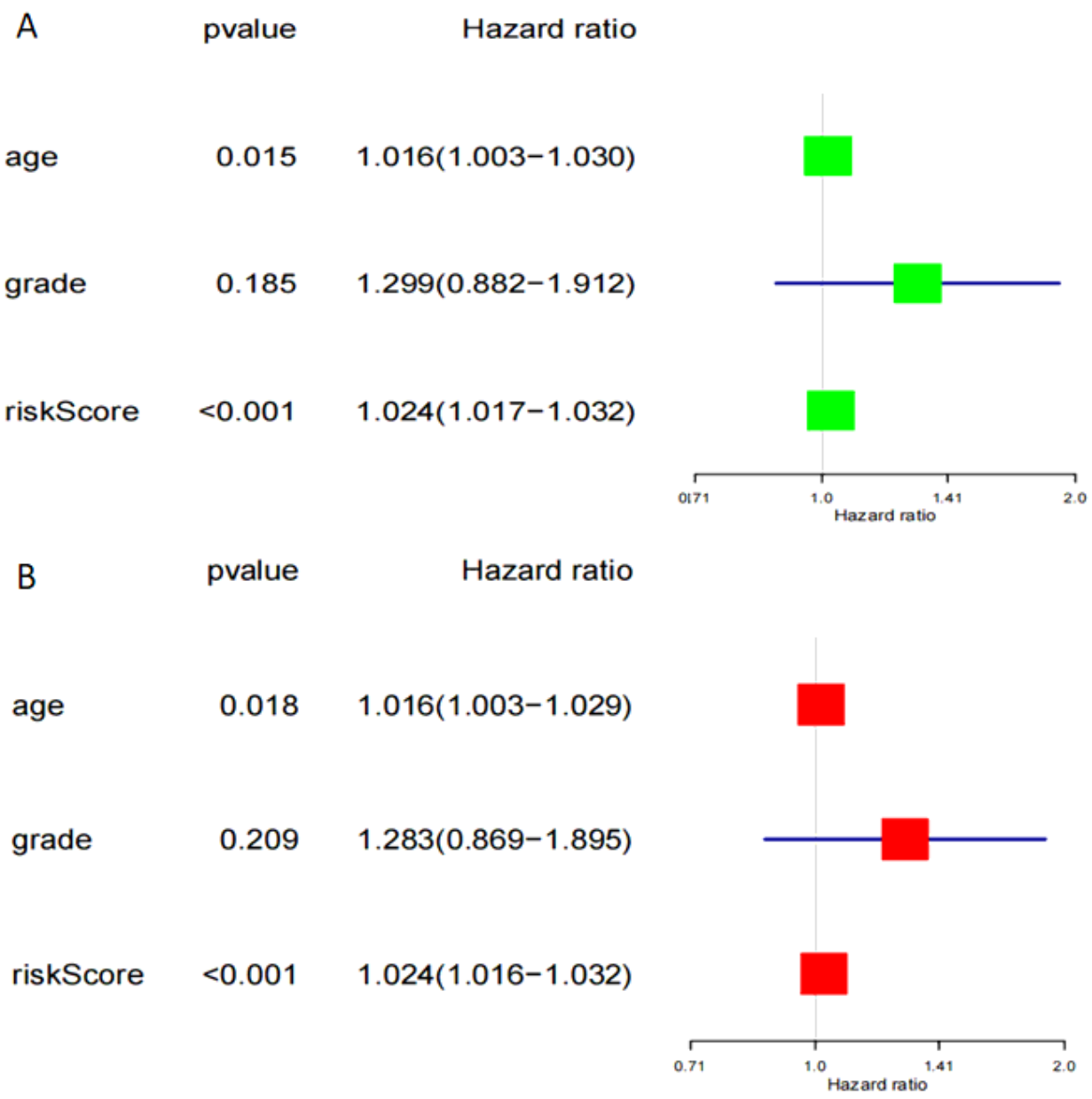

Figure 4

The prognostic value of age, stage, and risk score in OV. Univariate (A) and Multivariate Cox (B) regression analyses of the prognostic model.

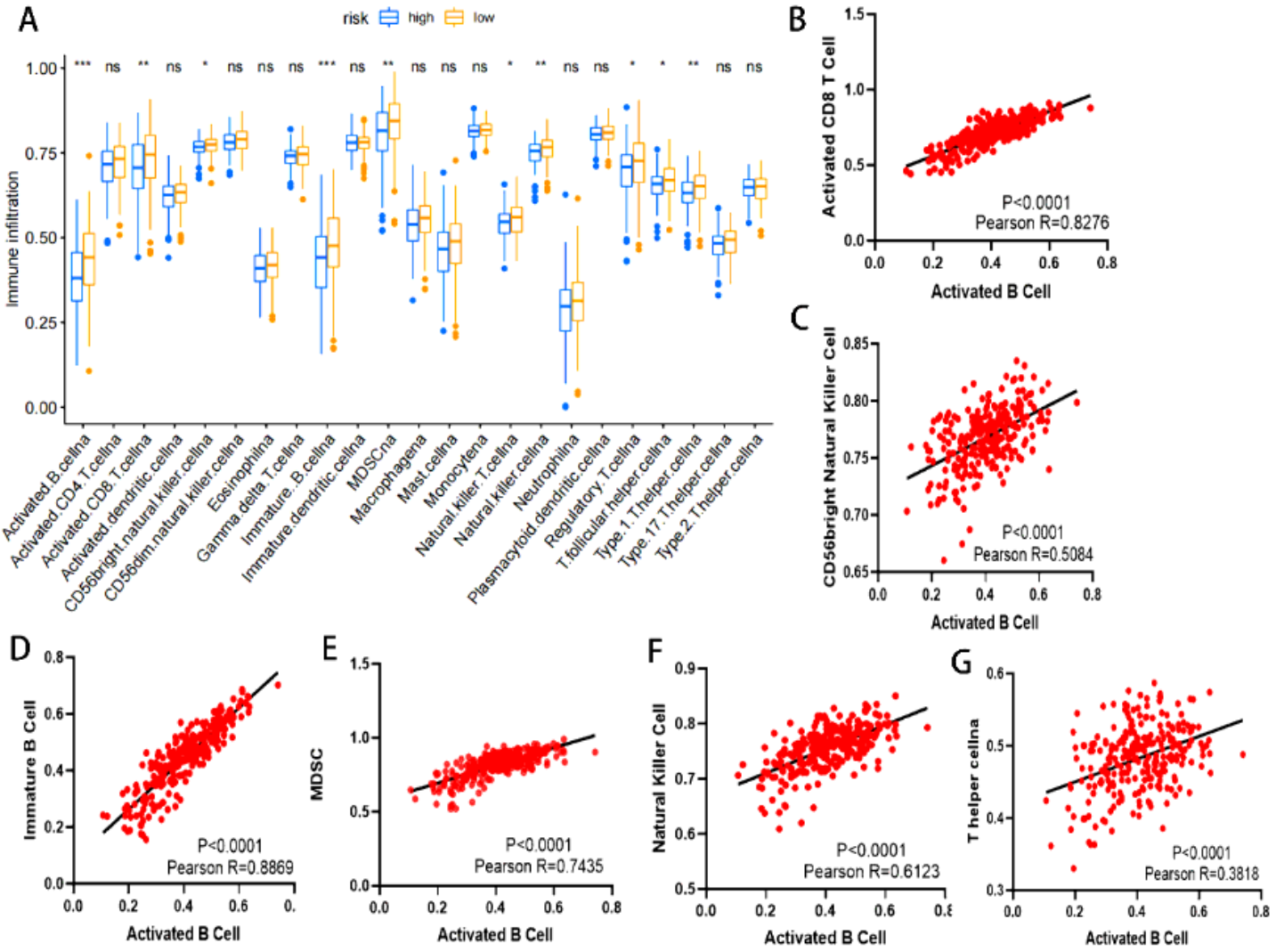

Figure 5

The riskscore is associated with the immune cells infiltrating in OV microenvironment. (A) Differences in the infiltrating proportion of 23 types of immune cells in two groups (low: 132 patients, high: 127 patients). (B) The correlation analysis showed that activated B cell was positively correlated with activated CD8 T cell, CD56 bright natural killer cell, immature B cell, MDSC, natural killer cell and type 1 T helper cell.

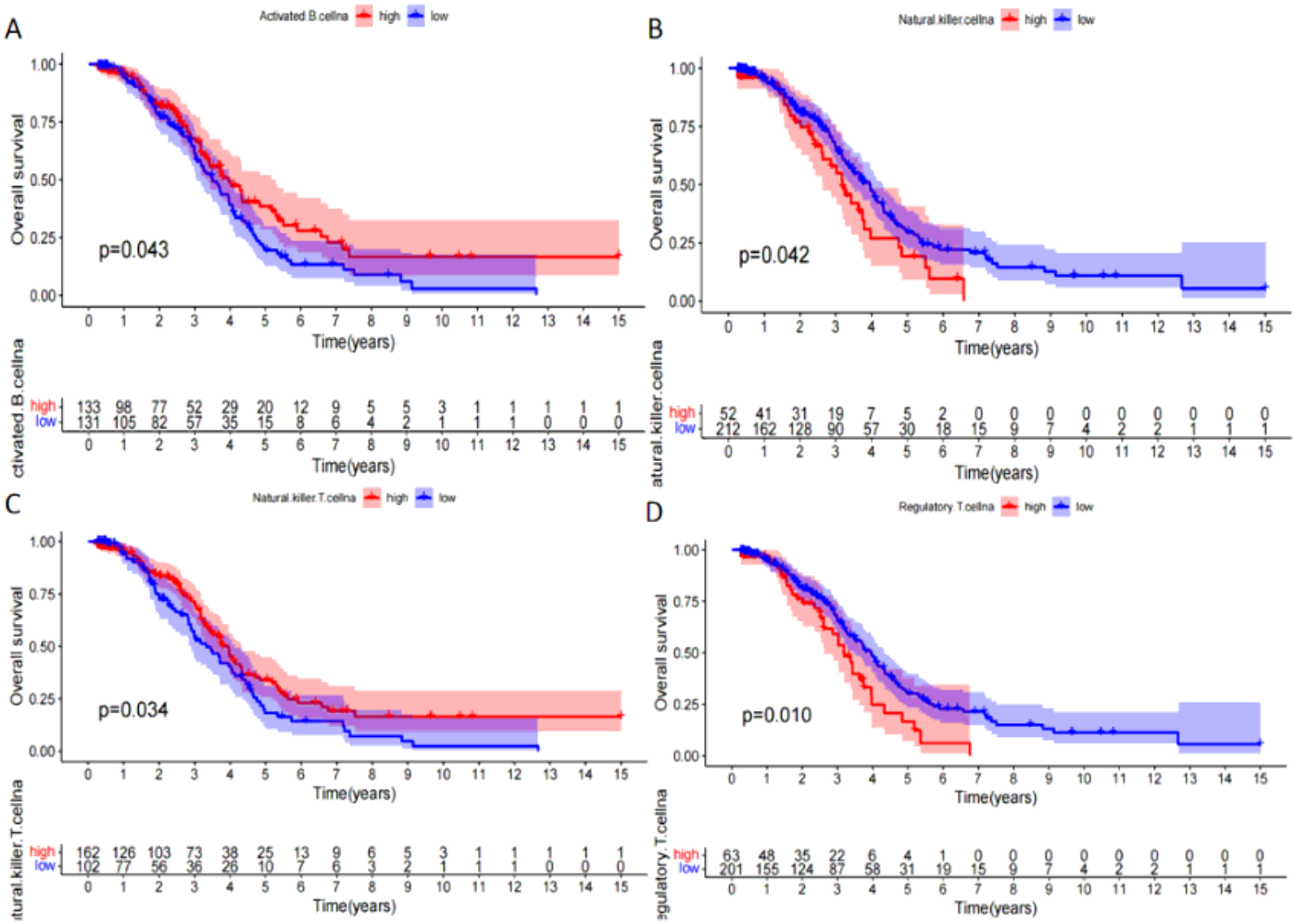

Figure 6

Kaplan–Meier survival curve of patients with survival-related immune cells. High expression of activated B cell (A) and natural killer T cell (C) was beneficial to the prognosis of patients, while natural killer cell (B) and regulatory T cell (D) was on the contrary.

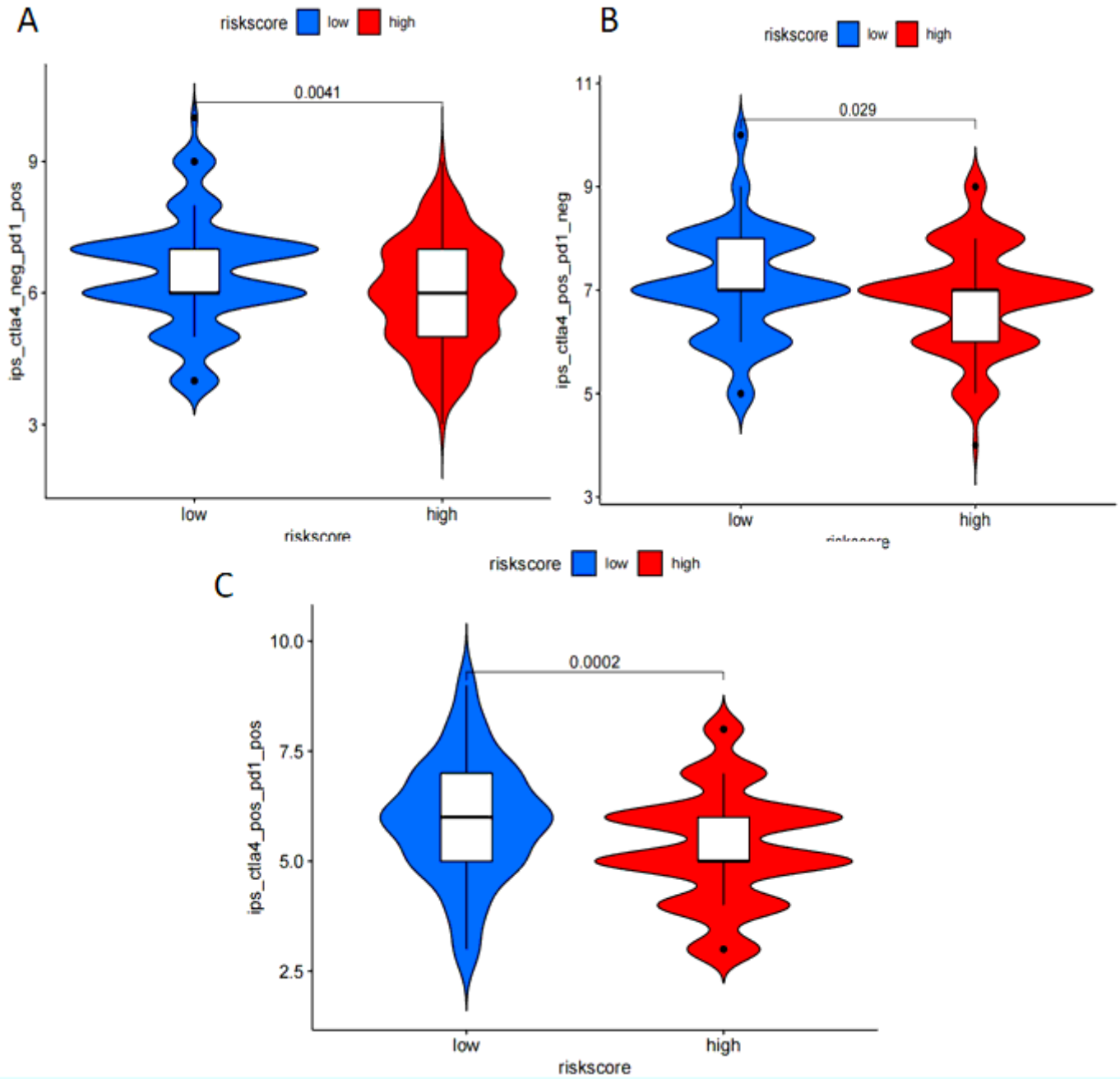

Figure 7

Violin diagram was used to visualize the different treatments (CTLA-4) response between low- and high-risk patients. The patients in low-risk group had good response to the single (A, B) and combined (C) use of the two drugs.

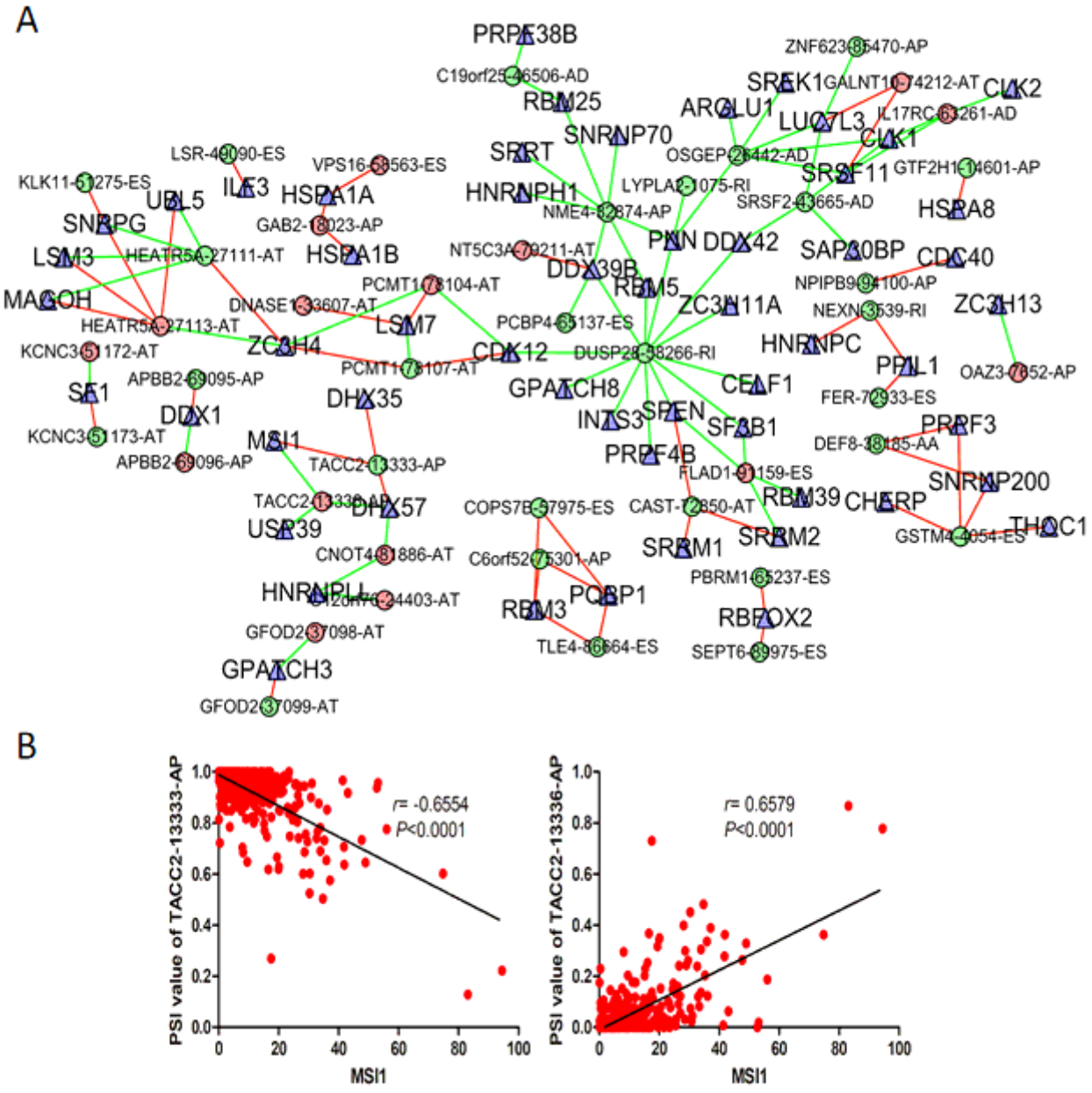

Figure 8

The interaction network and correlation between SFs and AS events. (A) The red dots indicate down-regulation, and the green dots indicate up-regulation. The blue triangles indicate SFs. The green lines represent AS events, which were positively correlated with the expressions of SFs, while red lines indicate negative correlations. (B) The correlation analysis was performed using Pearson t test. MSI1 could positively regulate -13336-AP (r=0.6579, P<0.0001) and negatively regulate TACC2TACC2-13333-AP (r=-0.6554, P<0.0001).

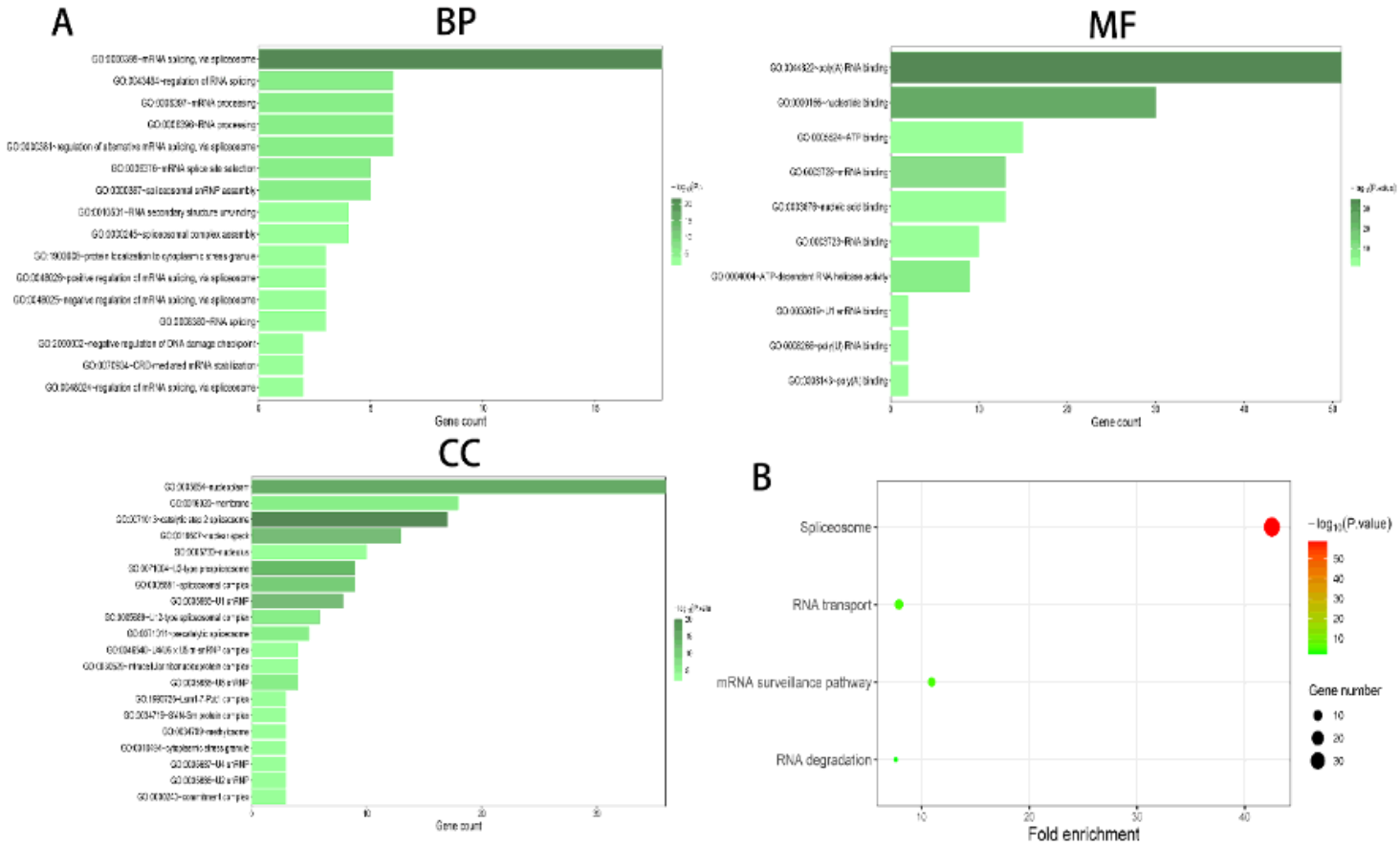

Figure 9

GO functional enrichment analysis (A) and KEGG pathway analysis (B)of AS event-related SF genes.

Supplementary Files

This is a list of supplementary files associated with this preprint. Click to download.

- Supplementarymaterial.pdf